

Downwind Performance of Yachts in Waves

Dougal Harris¹, Giles Thomas¹, Martin Renilson²

SUMMARY:

This paper reports on work conducted to date investigating the downwind performance of yachts in waves. The main objective of this research is to develop numerical models, resulting in computer software, that may be incorporated into a VPP to predict the mean velocity of a yacht when sailing downwind in waves. The software will be used to investigate how design parameters, such as hull and appendage shape and sail and rig configurations, affect the performance of yachts sailing downwind in waves.

The forces acting on the yacht to be investigated are as follows:

- wave induced longitudinal force.
- hull resistance forces.
- sail forces.

A numerical model has been developed for each of these forces and incorporated into a longitudinal motion time domain simulation. The simulation predicts the velocity, heave and pitch of the yacht. Experiments have been conducted at the Australian Maritime College's Ship Hydrodynamics Centre to validate the wave force and resistance numerical models. Experimental results have been compared with theory and conclusions drawn.

1. INTRODUCTION:

The investigation into the upwind performance of yachts in waves has been the focus of extensive yacht research since the 1970s. The outcome of such research has been incorporated into ocean racing handicapping systems such as the International Measurement System (IMS), and other Velocity Prediction Programs (Kerwin 1976, Oliver and Claughton 1995). To date little work has been carried out into the performance of yachts in following waves.

At present, designers have no tools for the systematic comparison of the performance of yachts sailing downwind in waves. The objective of this project is to develop computer software for use in the design, design selection and optimisation of high performance racing yachts. The developed computer code will predict the performance of yachts in following waves. This is an issue of particular importance to yacht design, as the speed differences between different designs travelling in following waves can be considerable. Many of today's high profile yacht races (Volvo 60, Around Alone) may spend the majority of the race sailing downwind in following waves. The prediction of speed differences between designs will assist in selecting the optimum design for a particular race or route.

This paper discusses the work carried out on the project to date and outlines its expected direction and outcomes.

2. PREVIOUS WORK:

When a vessel is accelerated to wave phase velocity, the vessel is said to be 'surf-riding'. Over the last two decades longitudinal wave induced forces have been the focus of researchers interested in the motions of large ocean vessels in following waves as well as those interested in the phenomenon of broaching-to of small fishing vessels (Renilson and Thomas 1991, Tuite and Renilson 1997).

¹Australian Maritime Engineering Cooperative Research Centre (AMECRC), Curtin University of Technology, Perth, Western Australia.

²Australian Maritime College (AMC), Launceston, Tasmania.

Du Cane (1957), conducted a series of following seas experiments on four different planing hulls from 'hard chine' to 'round form'. Tests were designed to demonstrate the value of the parameters important to the designer in forming a judgement on the seakeeping qualities inherent in the various hull forms. Free-running model experiments were conducted with radio controlled rudder adjustments and self propulsion at constant thrust.

Grim (1962) devised an experimental technique for the measurement of wave induced surging force in captive model experiments, using a quasi-static assumption. He carried out a number of experiments, at or close to wave celerity, to build a picture of the vessel's surging behaviour in all phases of a wave.

DeSaix (1968) performed a series of tests on two separate hull forms to determine the relative importance of hull parameters on surf riding ability. The tests were conducted in the free to surge condition so the relative surfing abilities of each hull could be compared.

Letcher (1977) suggested the surfing performance of a yacht could be determined from a series of flat water experiments while varying ballast conditions.

Sclavounos and Nakos (1993) developed a 3 dimensional panel method for determining the motions of ships in a sea way. This code (the Swan code) was later modified to account for 'non-linearities' introduced when trying to predict the performance of yachts in a following seaway. Falsone (1997) conducted a series of model experiments to verify results of the Swan code. Tests were conducted with the model fixed in surge and varying encounter frequency and appeared to agree with results obtained by Sclavounos and Nakos (1993). Analysis revealed that for wave lengths greater than approximately two hull lengths (for encounter frequencies ranging from 0.192 to 0.203) the added resistance due to a following seaway is negative, and as the wave length increases above five hull lengths the resistance converges to the still water resistance.

Kan (1990) formulated an expression for the longitudinal wave force using the Froude-Krylov hypothesis in the horizontal direction and linear wave theory. Using this hypothesis it was possible to identify critical vessel speeds and wave steepnesses that would lead to surf-riding. The theory was verified with free running, remote controlled model experiments.

Thomas and Renilson (1991) carried out model experiments of three different hull forms of a typical fishing vessel in following waves. The wave force was found to be a function of the vessel position in the wave at low encounter frequencies. The assumption that wave force is dependent on wave position only for low encounter frequencies is termed the "quasi-static" assumption. A method to predict the maximum wave force as a function of the wave steepness and midship area coefficient was proposed. The variation of longitudinal wave force with wave height was found to be approximately linear.

Keuning *et. al.* (1993) carried out similar experiments to Thomas and Renilson on three yacht hull forms from the Delft Systematic Series. Experiments were conducted at various wave lengths and steepnesses and compared with theory. The theory was calculated using the Froude-Krylov hypothesis using two different methods: i) integrating to the calm water line and ii) integrating over the instantaneous wetted surface area and taking into account sinkage and trim due to the high forward speeds. It was found that the second method resulted in better agreement with the experimental results.

Tuite and Renilson (1997) carried out captive model experiments and developed simulation software to identify surf riding and broaching zones as a function of wave steepness and heading angle for the 21m Success class trawler. The simulation software included the effect of forces induced by wave, wind, propeller, rudder and hull. The simulation involved a six degree of freedom time-domain non-linear mathematical model. Initial conditions for each simulation were found to have a significant effect on the simulation outcome and thus a method based on phase-plane and time-domain analysis was proposed. Simulations were carried out varying design parameters such as KG, draft, beam and rudder size to determine their effect on surf-riding ability and controllability (and hence likelihood of broaching-to).

3. OBJECTIVES

The objective of this research is to develop a numerical model for the prediction of downwind performance of yachts in waves. Two of the modules of the proposed numerical model have been validated by experiment and the results are presented in this paper.

The first set of experiments set out to verify the calm water resistance model. The second group of experiments were conducted to determine whether a numerical model, based on the Froude-Krylov theory and quasi-static assumption, would be appropriate to predict the relative wave forces on different

yacht hull forms in following waves. It was decided to conduct a similar set of test to that of Thomas and Renilson and Keuning *et. al.*

4. NUMERICAL MODEL

To predict the performance of a yacht operating in following waves a numerical model of the yacht's response to external forces and moments is being developed.

The present model takes into account forces induced by sails, hull and waves. These are resolved to obtain a total force. Using Newton's second law, the force is applied over a specified time interval (0.1 seconds), the resultant acceleration is used to determine the new velocity, position in wave and relative wind velocities.

Fig.1 indicates the coordinate system being employed:

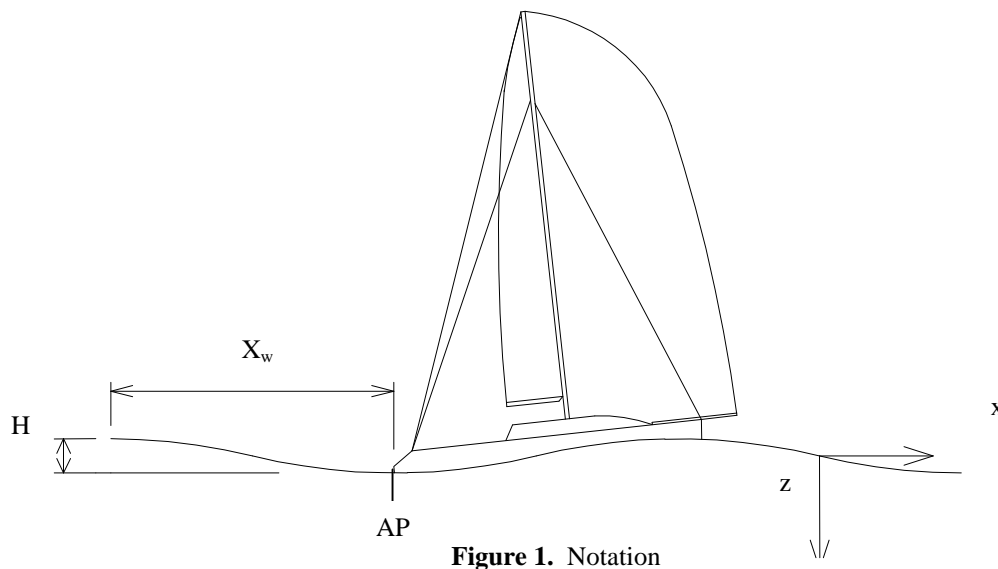


Figure 1. Notation

The longitudinal equation of motion adopted for the numerical model is shown below:

$$(m - X_u) \cdot \dot{u} = X_x(\xi) + R(u) + T(V_{wa}, \theta_a)$$

where X_ξ is the longitudinal wave force which is dependent on the yacht's non-dimensional position in the wave, ξ ; R is the resistance force and is dependent on the yacht velocity, u ; and T is the thrust provided by the sails and is dependent on the apparent wind velocity, V_{wa} , and relative wind angle, θ_a .

A method for calculation of calm water resistance has been extensively studied both experimentally and theoretically at Delft University of Technology (Gerritsma *et al.* 1992, Keuning *et al.* 1998). Computer code has been developed to calculate the upright calm water resistance according to Gerritsma *et al.* (1992).

The input parameters to the computer code are canoe body hull offset table; waterline length; canoe body draft; keel wetted surface area and mean chord length; and rudder wetted surface area and mean chord length. The total resistance is calculated from the addition of the residuary resistance and frictional resistance (ITTC 1957):

$$R_t = R_r + R_f$$

The residuary resistance is determined analytically using a polynomial equation with hull form geometry coefficients as variables (Gerritsma 1991):

$$R_r / \Delta_c \times 10^3 = A_0 + A_1 C_p + A_2 C_p^2 + A_3 LCB + A_4 (LCB)^2 + A_5 B_{WL} / T_c + A_6 L_{WL} / \nabla^{1/3}$$

The coefficients $A_0 - A_6$ are given in tabular form as a function of Froude number.

The frictional resistance for yachts is calculated by adding the contributions from keel, rudder and canoe body:

$$R_f = 1/2 \rho u^2 (S_c C_{Fc} + S_k C_{Fk} + S_r C_{Fr})$$

where S_c, S_k and S_r are the wetted surface areas of the canoe body, the keel and the rudder respectively. The terms C_{Fc}, C_{Fk} and C_{Fr} are the corresponding frictional resistance coefficients. These coefficients are calculated accordingly using the ITTC (1957) formulation:

$$C_F = \frac{0.075}{(\log R_n - 2)^2}$$

where Reynolds numbers are determined separately for canoe body, keel and rudder:

$$R_{nc} = \frac{0.7 \times V \times L_{WL}}{n}$$

$$R_{nk} = \frac{V \times \bar{C}_k}{n}$$

$$R_{nr} = \frac{V \times \bar{C}_r}{n}$$

and \bar{C}_r and \bar{C}_k are the average chord length of the rudder and keel.

The average length for a typical profile of the canoe body of a yacht is defined by the ITTC as $0.7 \times L_{WL}$.

Wave induced forces and moments on a yacht in following waves are extremely complex. To simplify the problem a quasi-static assumption produces forces and moments as a function of the yacht's position in the wave only.

The predominant longitudinal force induced by the wave is the Froude-Krylov force. Due to the very low encounter frequency diffraction forces may be ignored. Computer code has been developed to calculate the longitudinal wave induced Froude-Krylov force, the input includes an offset table of the canoe body along with wave length, amplitude and water density.

The Froude-Krylov forces arise from the undisturbed pressure field acting on the submerged surface of the hull, given by (Umeda, 1984):

$$X(\mathbf{x}) = -\rho g z k \int_{FP}^{AP} e^{-kd(x)} S(x) \sin k(\mathbf{x} + x) dx$$

where $S(x)$ is the sectional area at a distance x . Using linear seakeeping theory, the wave pressure is assumed to act up to the calm water free surface position, as the wave height is assumed to be small. The developed program at this stage calculates the force on the canoe body with no keel or rudder appendages.

Only the longitudinal force is calculated at this stage. The wave induced sway force and yaw and roll moments are somewhat more complicated to calculate as the Froude-Krylov forces are not so dominant and diffraction forces must be effectively accounted for.

A preliminary sail force model proposed by Hazen (1980) is used in the initial sail force computer code. This model, with minor alterations, is used in many VPPs, for example the IMS handicap system.

When sailing directly downwind all thrust provided from the sail is purely from drag. Hence the sail thrust is given by:

$$T(V_{wa}) = 0.5 \cdot r_a \cdot V_{wa}^2 \cdot C_D$$

where V_{wa} is the apparent wind velocity and r_a is the air density:

$$\text{Area of main : } A_M = 0.5 \cdot P \cdot E$$

$$\text{Area of jib : } A_J = 0.5 \sqrt{I^2 + J^2} \cdot LPG$$

$$\text{Area of spinnaker : } A_S = 1.15 \cdot SL \cdot J$$

$$\text{Area of foretriangle : } A_F = 0.5 \cdot I \cdot J$$

$$\text{Nominal Area : } A_N = A_F + A_M$$

Viscous Drag:
$$C_{DP} = \frac{C_{DPM} \cdot A_M + C_{DPJ} \cdot A_J + C_{DPS} \cdot A_S}{A_N}$$

Induced Drag:
$$C_{DI} = C_L^2 \cdot \left(\frac{1}{p \cdot AR} + 0.005 \right) \left\{ \begin{array}{l} \text{close hauled} = \frac{(1.1 \cdot (EHM + FA))^2}{A_N} \\ \text{other courses} = \frac{(1.1 \cdot EHM)^2}{A_N} \end{array} \right.$$

Drag of mast and topsides:

$$C_{DO} = 1.13 \cdot \frac{(B \cdot FA) + (EHM \cdot EMDC)}{A_N}$$

Total drag:
$$C_D = C_{DP} + C_{DI} + C_{DO}$$

Drag force:
$$DRAG = 0.5 \cdot r \cdot v_a^2 \cdot A_N \cdot C_D$$

when sailing directly downwind ($b=180^\circ$):

Drive force:
$$\text{Drive force} = LIFT \cdot \sin b + DRAG \cdot \cos b = DRAG$$

Side force:
$$\text{Side force} = LIFT \cdot \cos b - DRAG \cdot \sin b = 0$$

Coefficients of lift, C_L , and viscous drag, C_D , are given for each of the main, jib and spinnaker sails as a function of apparent wind angle. An example output from the computer code is given in Fig. 2

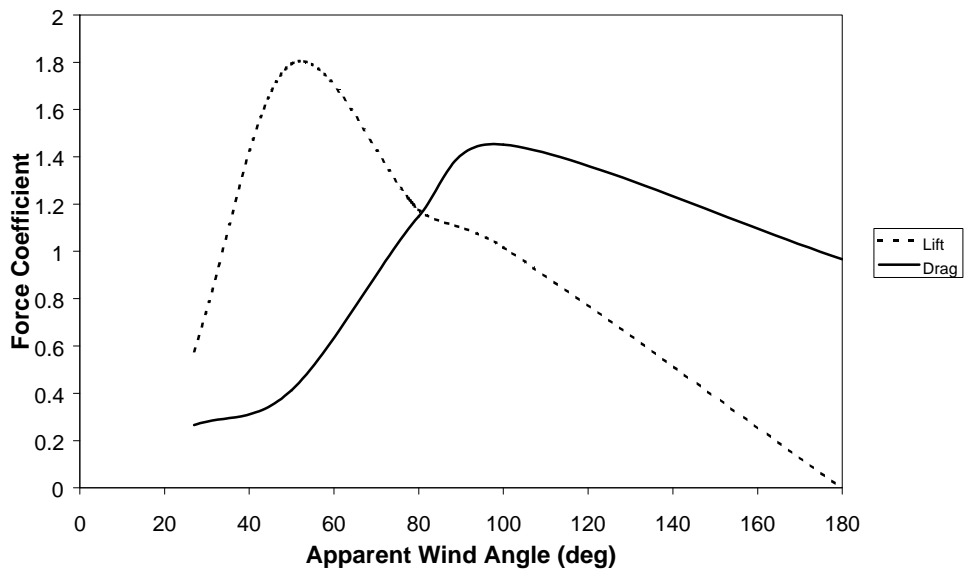


Figure 2. Sail lift and drag coefficients versus apparent wind angle.

With all the forces effectively accounted for it is possible to construct a numerical simulation. The flow chart in Fig. 3 indicates the logic:

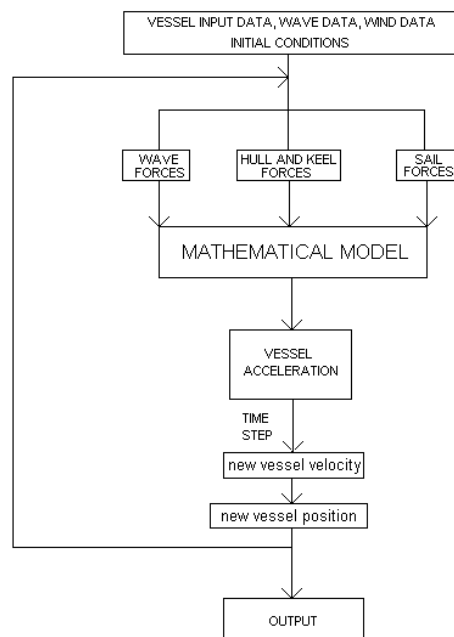


Figure 3. Numerical simulation flow chart.

The two simulations combined into Fig.4 illustrate the yacht's behaviour under two different wave conditions. Both simulations begin with the same true wind velocity and at the same position in the wave, $\xi=0$ (AP on wave crest).

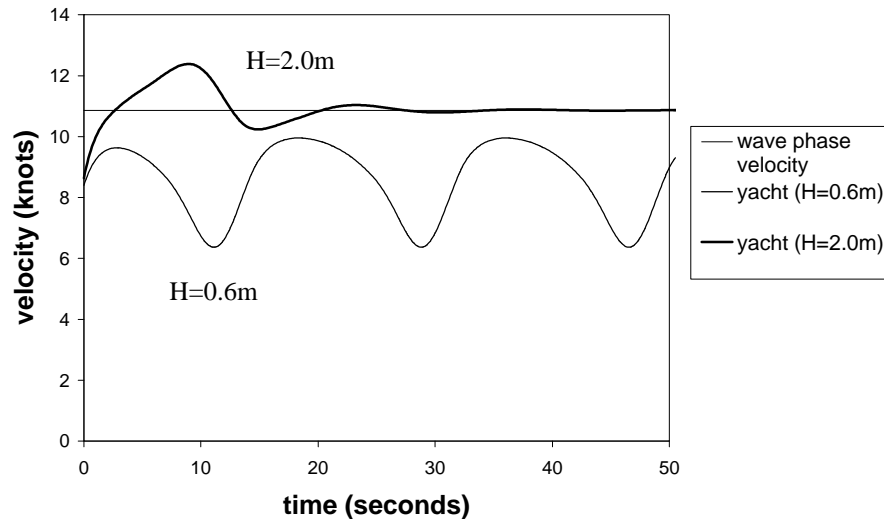


Figure 4. Example Simulation; AME 004, $\lambda=20.0\text{m}$, $V_w=15$ knots

The velocity of the yacht in the wave height of 0.6m fluctuates periodically as it moves through different positions in the wave. In this case the wave is overtaking the yacht; when the yacht is travelling fastest it will be closest to wave celerity and will hence spend more time in this section of the wave.

When the wave height is increased (2.0m) the wave force is increased sufficiently to accelerate the yacht's velocity to wave celerity. In this instance the yacht's longitudinal position in the wave reaches a stable equilibrium. This is known as surf-riding. The yacht's velocity is significantly increased over its calm water velocity under the same wind conditions. Simulation results are sensitive to the vessel's initial position in the wave, therefore when comparing different simulations care must be exercised to ensure that the initial conditions are identical.

5. EXPERIMENTS:

Experiments were conducted to validate the wave force and resistance force models used in the numerical model for three different underwater hull forms. Experiments were conducted in the towing tank at the Ship Hydrodynamics Centre of the Australian Maritime College. The towing tank is 60m long, 3.5m wide and 1.5m deep. The experiments conducted were semi-captive using a dual post system with the model free to heave and pitch while being constrained in surge, sway, yaw and roll. Measurements of heave, pitch, surge force and sway force were taken. A wave probe was positioned one wave length in front of the AP to determine the model's relative position to the wave, and a stationary wave probe was used to measure the wave height and profile. The data was recorded by a PC at a sampling frequency of 100 Hz for 10 seconds.

The model used for experiments was the parent hull, 004, of the AME CRC systematic yacht hull series, Fig. 5.

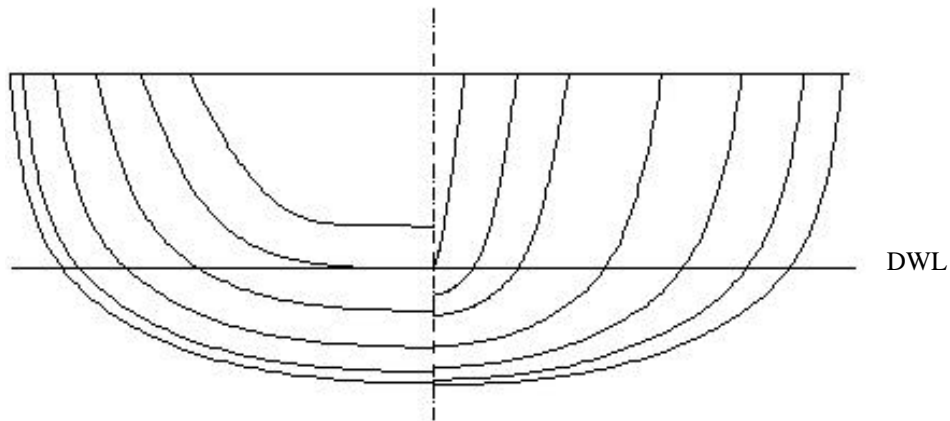


Figure 5. Body plan AME 004.

Assuming deep water wave theory the maximum wave length attainable, without distortion and a water depth of 1.5m, was 3.0m. With this restriction a model length of 1.5m was chosen to allow experiments to be conducted at $\lambda/LWL=2.0$. Particulars of the full scale yacht hull form are presented in Table I.

	AME 004
Length W.L.	10.0m
Beam W.L.	2.654m
Draft (canoe body)	0.417m
Displacement	4.405t
Prismatic Coefficient	0.532
LCB (aft of FP)	-5.597m
LCF (aft of FP)	-5.666m
Model Scale	1:6.667

Table I. Full scale AME 004 hull principle particulars

The experimental test matrix is outlined in Fig. 6.

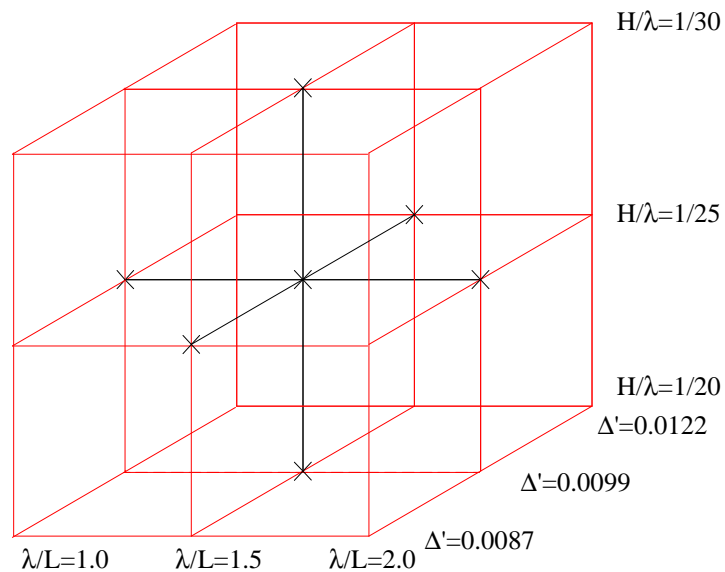


Figure 6. Test matrix (X = conditions tested).

6. RESULTS AND DISCUSSION:

The longitudinal wave force was determined by subtracting the calm water resistance from the overall drag measured:

$$X_x = X_M - R(u)$$

where X_M is the total measured force on the model and $R(u)$ the calm water resistance. Calm water results are presented in Fig. 7 and compared with theory:

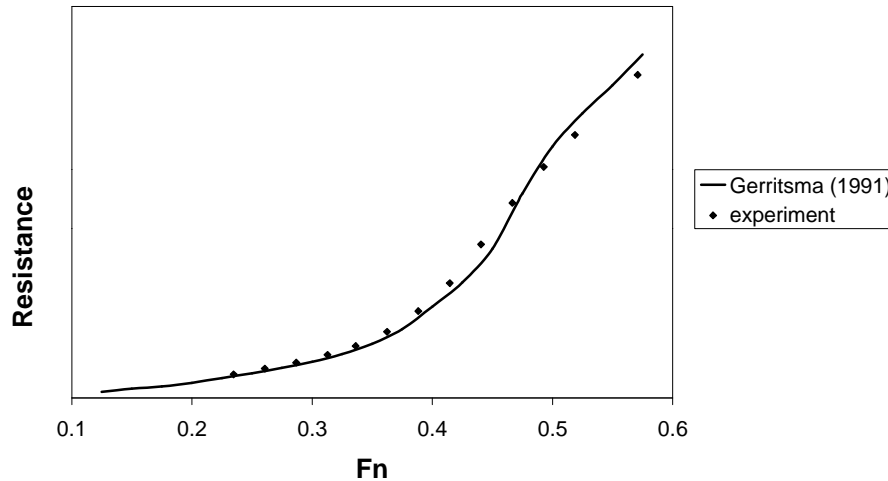


Figure 7. Upright Calm Water Resistance; AME 004, LWL=1.5m

As may be seen in Fig. 7 calm water resistance results compared extremely well with theory. The theory proposed by Gerritsma (1992) does not account for trimming moments induced by the sail. Initially a trimming moment was added to the model during the wave experiments, however this led to nose diving problems. Therefore no trimming moment was applied to the model during either the wave or calm water experiments. Whilst necessary from a practical standpoint, this may be assumed to be acceptable since when sailing downwind in large waves the crew weight would be moved aft and there may be considerable vertical lift from the spinnaker, therefore providing only a small net trimming moment.

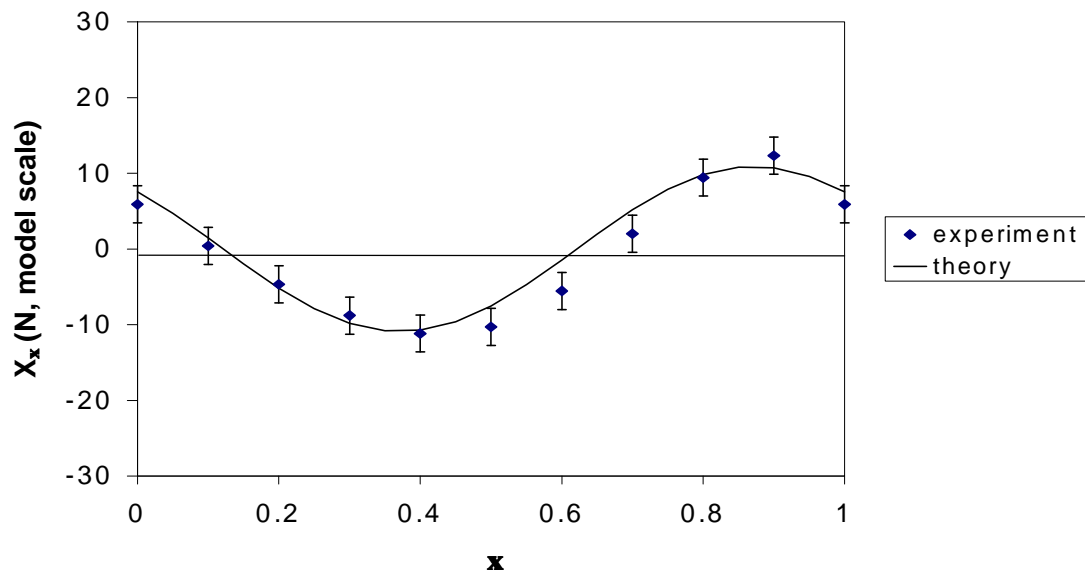


Figure 8. Wave Force versus ξ ; AME 004, $\Delta'=0.0099$, $H/\lambda=1/25$, $\lambda/LWL=1.5$, $u/C_w=0.85$

Fig. 8 shows the variation of non-dimensional wave force with wave position both experimentally and theoretically. Correlation between the theory and experiment is satisfactory. Error bars on the graph indicate that 95% of the data points from the experiment lie within this region. The longitudinal wave induced force is periodic over the wave length and the peak force occurs when the yacht is on the front face of the wave (ξ).

The first tests conducted were for a range of encounter frequencies to validate the quasi-static assumption. A cross plot of $X_{\xi_{peak}}$ against u/C_w is presented in Fig. 9.

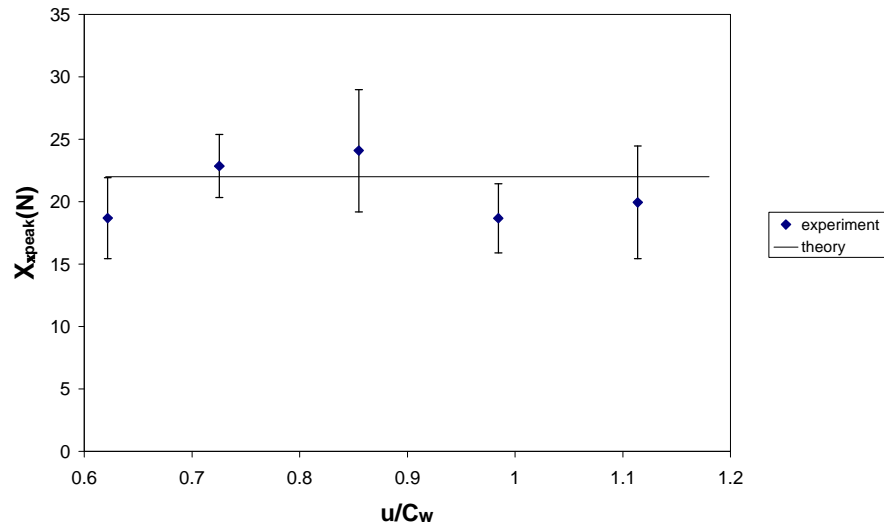


Figure 9. Wave Force (peak to peak) versus Encounter Frequency; AME004, $H/\lambda=1/25$, $\lambda/LWL=1.5$, $\Delta'=0.0099$

where $X_{\xi_{peak}} = X_{\xi_{max}} - X_{\xi_{min}}$. From Fig. 9 it was apparent that encounter frequency had a negligible effect on the wave force for the range tested. This implies that it is valid to use the quasi-static assumption for the simulation provided the encounter frequency lies within the tested limits. To determine the $X_{\xi_{peak}}$ value for $u/C_w=1$, 20 separate runs were conducted with the model at different positions in the wave. It was decided to conduct further experiments at a u/C_w of 0.86. This allowed a full wave length to overtake the model per run, greatly reducing the runs required for each condition.

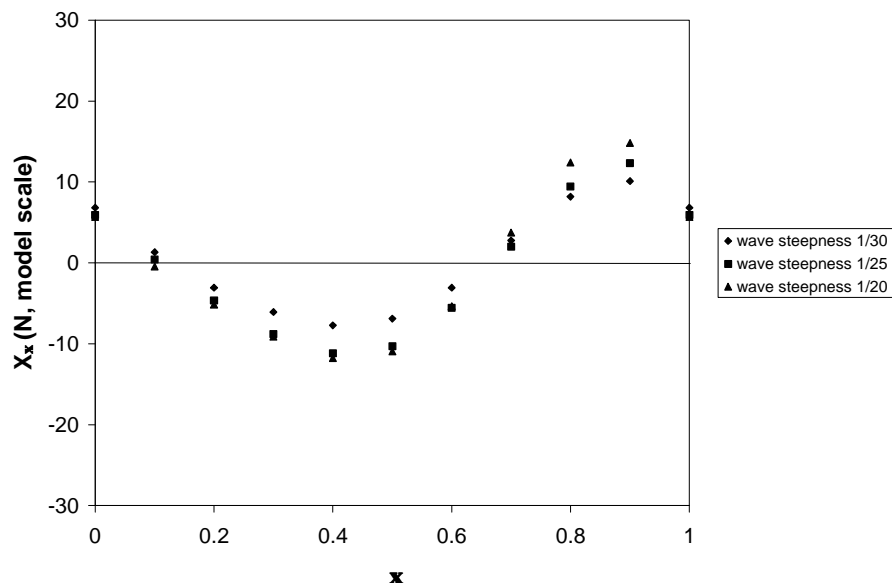


Figure 10. Wave Force versus ξ ; AME 004, wave length = 2.25m

Fig. 10 indicates the longitudinal wave force versus wave position for different wave heights. As expected the model experiences greater longitudinal wave force at higher wave height. Maximum wave force occurs when the crest is just forward of the aft perpendicular ($\xi=0.9$).

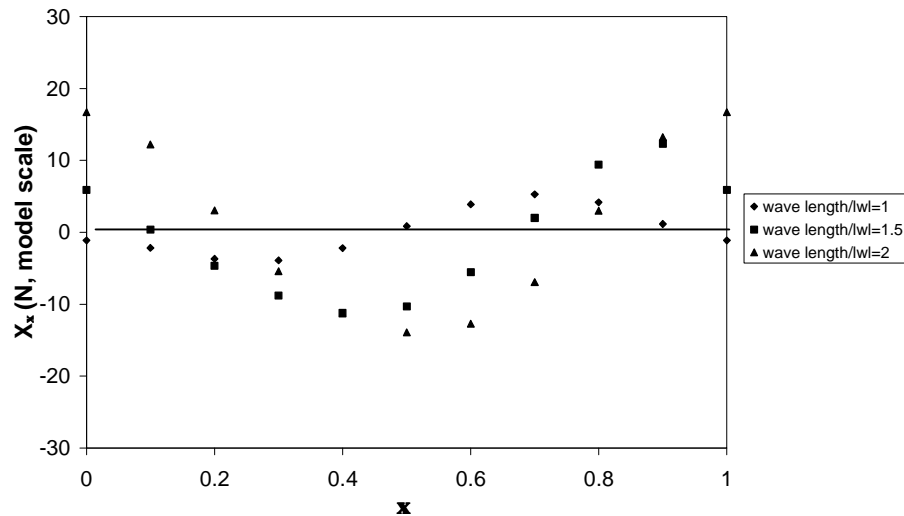


Figure 11. Wave Force versus Wave Position; AME 004, $H/\lambda=1/25$

Fig. 11 indicates the longitudinal wave force versus wave position for different wave lengths. The amplitude increases with wave length; however, because steepness is constant wave height also increases. The position of the maximum wave force shifts with wave length, due to the change in relative length of the hull compared to the wave length. In the case of the wave length equal to twice the vessel length, maximum wave force occurs when the entire hull is on the front of the wave (i.e. $\xi = 0$). In the case of the wave length equal to 1.5 times the vessel length the maximum wave force occurs when the wave crest is just forward of the AP, this corresponds to midships being on the front face of the wave ($\xi=0.85$).

Fig. 12 shows the variation of wave force with wave steepness and wave length.

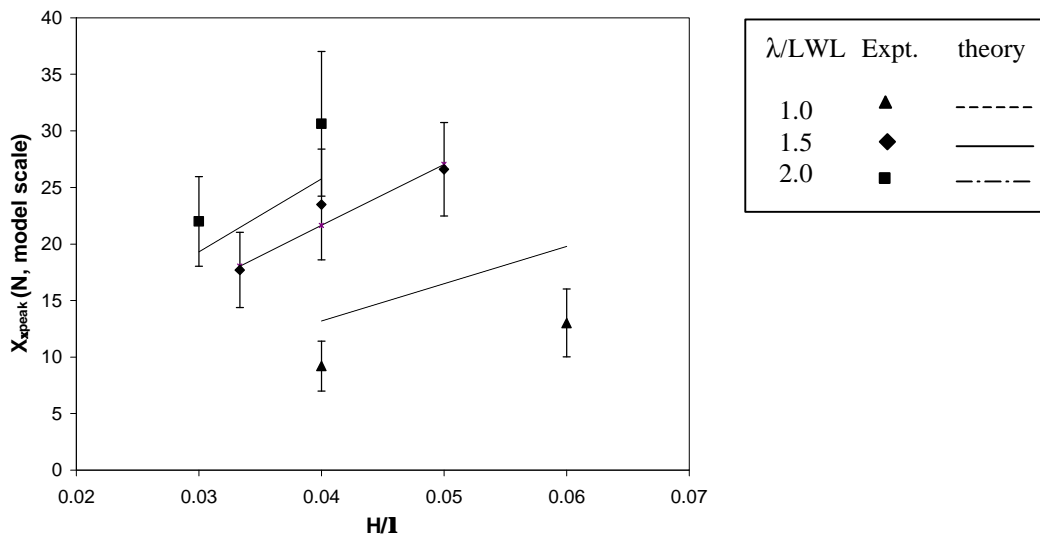


Figure 12. Wave Force versus Wave Steepness for different λ/LWL ; AME004, $\Delta'=0.0099$, $u/C_w=0.85$

Fig. 12 indicates that as wave steepness increases the wave force increases. At constant steepness, as the wave length increases the wave force also increases. The theory appears to predict wave forces with the greatest degree of accuracy at the middle and longer wave lengths. During ocean races yachts will tend to encounter wave lengths greater than 40m. A yacht in the Volvo 60 around the world yacht race, on average will spend 75% of its time sailing downwind in swells of wave length greater than 40m ($\lambda/LWL=2$) in the Southern Indian Ocean, Hogben and Lumb (1967).

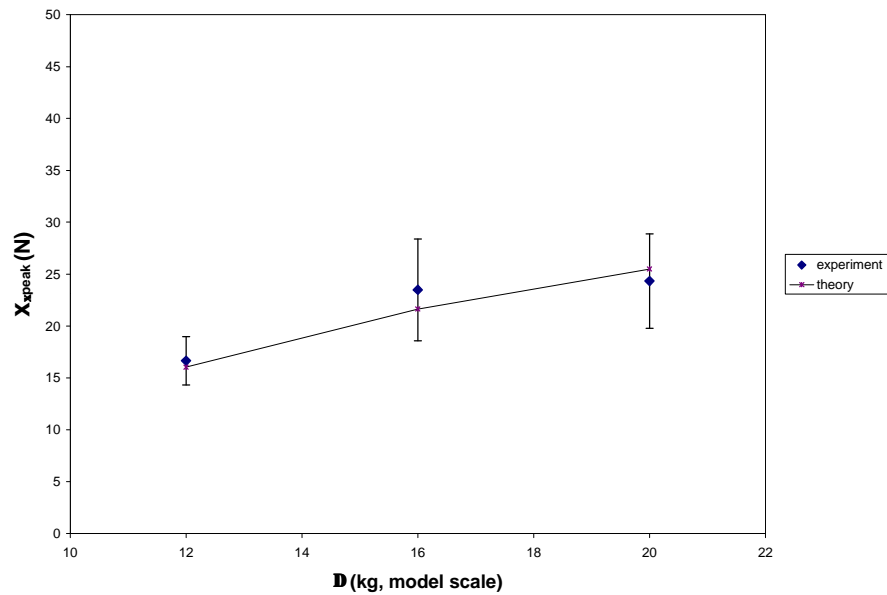


Figure 13. Wave Force versus Displacement; AME004, $\lambda/LWL=1.5$, $H/\lambda=1/25$, $u/C_w=0.85$

Fig. 13 shows the wave force variation with displacement, and as expected at large displacements (hence larger submerged volume) the wave force is greater. From the experimental results the gradient of the increase in wave force changes with displacement - this corresponds to the numerical results. This indicates that for this style of hull form the theory is able to predict the change in wave force due to a change in submerged hull form.

If the wave force is non-dimensionalised (as outlined below) with respect to wave height, then the experimental points, including the models of different displacements, tend to collapse onto each other

(Fig. 14). This suggests that the wave force is dependent on the wave height and midship area coefficient (A_m).

$$X_x' = \frac{X_x}{0.5 \cdot r \cdot \sqrt{A_m} \cdot H \cdot C_p^2}$$

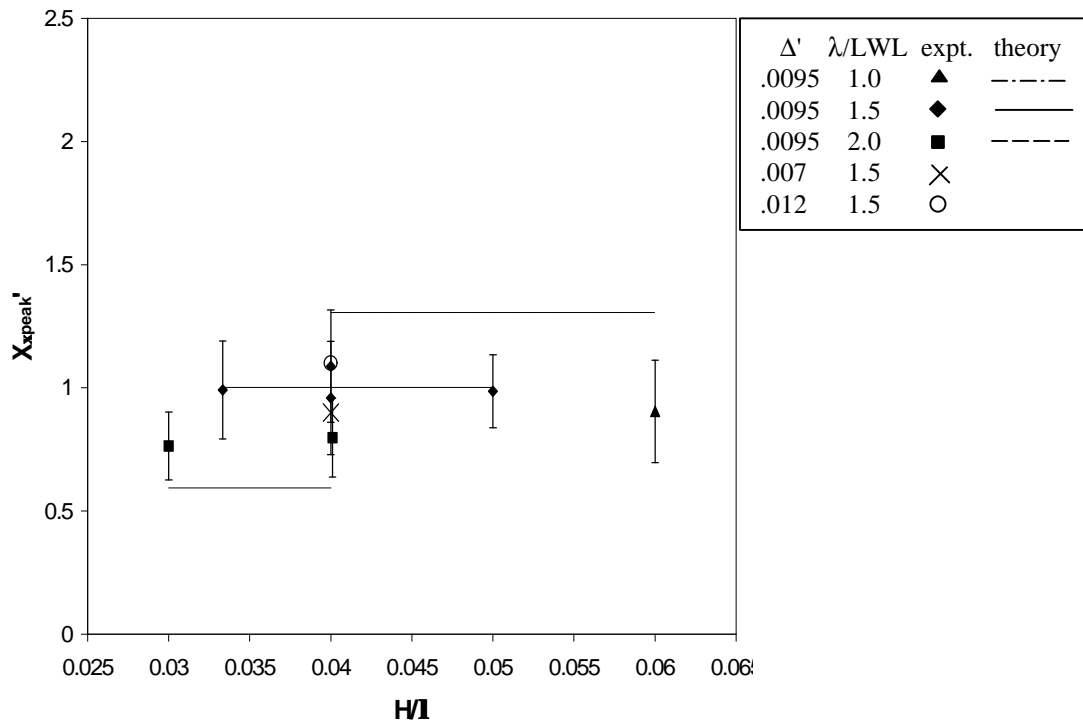


Figure 14. Wave Force versus Wave Steepness for different λ/LWL ; AME004, $\Delta'=0.0099$, $u/Cw=0.85$

The discrepancies between theory and experiment have been compared with previous work conducted on fishing trawlers, Fig. 15.

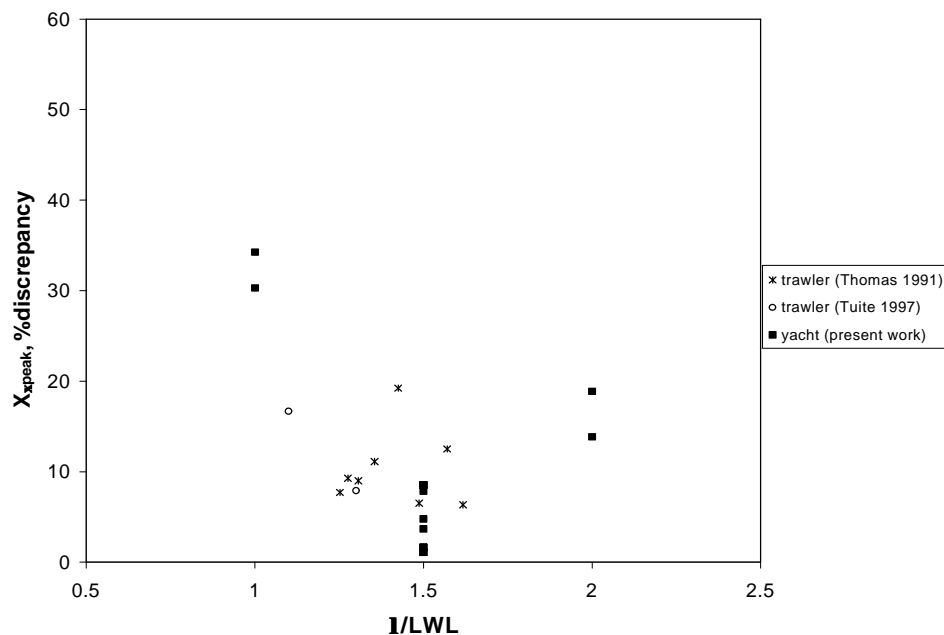


Figure 15. % discrepancy (between theory and experiment) versus λ/LWL for different λ/LWL

Where $X_{\xi peak}$, %discrepancy = $(X_{\xi theory} - X_{\xi experiment}) / X_{\xi theory}$. At the middle wave length the present theory predicts the wave force exceptionally well. At the higher wave length error increases but is comparable with discrepancies found by Thomas and Renilson (1991) and Tuite (1997). For wave lengths equal to ship length the error is the greatest; this may be due to inherent assumptions made when using the Froude-Krylov hypothesis, as outlined earlier. The assumption that the wave height is small and hence only integrating to the calm water line of the vessel is clearly violated when the wave amplitude is of the magnitude of the canoe body draft of the hull. This problem is not so evident with

fishing trawlers, having a much greater draft than the canoe body of a yacht hull form. The yachts also have significant stern and bow overhangs, which may be submerged when the wave is present but is not accounted for when only integrating to the still water line. Future additions to the code will include determining the wave force integrating to the dynamic wetted surface area.

7. CONCLUSIONS

A numerical model has been developed to simulate the downwind performance of a specified yacht hull shape in waves. The resistance and wave force components of this model have been verified with experimental results. For the model tested:

1. The longitudinal wave induced force is periodic over the wave length and the peak force occurs when the yacht is on the front face of the wave.
2. The longitudinal wave force increases with wave height.
3. The wave force is independent of encounter frequency over the range of encounter frequencies tested ($0.63 < u/C_w < 1.12$).
4. The numerical model predicts the change in wave force due to a change in underwater hull form.
5. The calm water resistance numerical model appears appropriate.

8. NOMENCLATURE

A_{0-6}	coefficients in resistance model	k	wave number
A_M	area main sail	LCB	longitudinal centre of buoyancy
A_J	area jib	LPG	perpendicular of longest jib
A_S	area spinnaker	LWL	waterline length
A_F	area foretriangle	m	mass
A_M	midship sectional area	P	main luff length
A_N	nominal sail area	R_f	frictional resistance
AP	aft perpendicular	R_n	Reynolds number
B_{wl}	waterline beam	R_{nc}	Reynolds number, canoe body
B	maximum beam	R_{nk}	Reynolds number, keel
C_D	drag coefficient	R_{nr}	Reynolds number, rudder
C_{DI}	induced drag coefficient	R_r	residuary resistance
C_{DO}	mast and topsides drag coefficient	R_t	total calm water resistance
C_L	lift coefficient	S_c	wetted surface area, canoe body
C_P	prismatic coefficient	S_k	wetted surface area, keel
C_{DP}	coefficient of viscous drag	S_r	wetted surface area, rudder
C_{DPM}	coefficient of viscous drag main	SL	spinnaker luff length
C_{DPJ}	coefficient of viscous drag jib	T	aerodynamic thrust provided by sails
C_{DPS}	coefficient of viscous drag spinnaker	\dot{u}	acceleration in x direction
C_w	wave phase velocity	u	velocity in x direction
\bar{c}_r	average rudder chord length	v	velocity in y direction
\bar{c}_k	average keel chord length	V_{wa}	apparent wind velocity
E	main foot length	V_w	true wind velocity
EHM	effective height of mast	X	surge force
$EMDC$	average mast diameter	X_u	added mass in x direction
FA	average freeboard	X_x	surge force as a function of wave pos.
FP	fwd perpendicular	X_{xpeak}	peak to peak surge force
g	gravity	Y	sway force
H	wave height	b	apparent wind direction
I	height of foretriangle	Δ_c	canoe body displacement
J	foot length of foretriangle	Δ'	non dimensional displacement
IMS	international measurement system		

ρ	water density	q_a	apparent wind angle
ρ_a	air density	x	distance from wave crest to transom
∇_c	volume of canoe body	λ	wave length
μ	viscosity of water	ν	viscosity
q	wind angle	Z	wave amplitude

Non-dimensionalisation methods:

- | | | |
|----|--------------------------|---|
| 1. | Displacement | $\Delta' = \frac{\Delta}{0.5 \cdot \rho \cdot L^3}$ |
| 2. | Wave induced surge force | $X_x' = \frac{X_x}{0.5 \cdot \rho \cdot \sqrt{Am} \cdot H \cdot C_p^2}$ |
| 3. | Calm water resistance | $C_t = \frac{\text{Resistance}}{0.5 \cdot \rho \cdot S \cdot V^2}$ |
| 4. | Vessel velocity | $Fn = \frac{V}{\sqrt{g \cdot lwl}}$ |
| 5. | Vessel position in wave | $x = \frac{\text{distance from wave crest to AP}}{\text{wave length}}$ |

8. REFERENCES

Abbot, I. and von Doenhoff, A. (1949),
 "Theory of Wing Sections"
 New York: McGraw Hill.

Acevedo, M.L., Mazarredo, L., Editors (15-23 September 1957)
 Eighth International Towing Tank Conference, Proceedings, Madrid.

DeSaix, P. (1968),
 "Model studies of two 30' W.L. cruising yachts"
 Davidson Laboratory, Hoboken, New Jersey.

Du Cane, P. (1957),
 "Model evaluation of four high speed hull forms in following and head sea conditions"
 Proceedings, Symposium on behaviour of ships in a seaway.

Falsone, J. (1997),
 "Model Tests of the PACT Base America's Cup Hull in Following Seas"
 SNAME 13th CSYS, Annapolis, M.D.

Grim O.K. (1962),
 "Surging motion and broaching tendencies in severe following seas"
 Davidson Laboratory Report R-929.

Gerritsma, J., Keuning, J.A. and Onnink, R. (1991)
 "The Delft Systematic Series II experiments",
 10th Chesapeake Sailing Yacht Symposium, Annapolis.

Hazen G.S. (1980),
 "A model of sail aerodynamics for diverse rig types",
 New England Sailing Yacht Symposium.

Hogben and Lumb (1967),
 "Ocean Wave Statistics", LONDON : Her Majesty's Stationary Office.

- Kan M.(1990),
"A guideline to avoid the dangerous surf-riding"
4th International Conference on Stability of Ships and Ocean Vehicles.
- Kerwin J.E. (1976),
"A velocity Prediction Program for Ocean Racing Yachts",
SNAME New England Sailing Yacht Symposium. Connecticut U.S.A.
- Keuning, J.A., Van Terwisga, P.F., Adegeest, L.J.M. (1993),
"Experimental and Numerical Investigation into the Wave Exciting Forces in Large Following Seas"
Laboratory of Shiphydrodynamics, Delft University of Technology, Netherlands.
- Letcher, J. (1977),
"Surfing - Motion of a Vessel Running in Large Waves"
SNAME, 3rd CSYS, Annapolis, M.D.
- Oliver, J.C., Claughton, A.R., (1995)
"Development of a Multifunctional Velocity Prediction Program (VPP) for Sailing Yachts"
CADAP '95, Southampton, U.K.
- Renilson M. and Thomas G. (1991),
"Surf-Riding and Loss of Control of Fishing Vessels in Severe Following Seas"
R.I.N.A., Spring meetings, London.
- Sclavounos, P.D. and Nakos, D.E. (1993),
"Seakeeping and Added Resistance of IACC Yachts by a Three-Dimensional Panel Method"
SNAME 11th CSYS, Annapolis M.D.
- Tuite, A. (1997)
"Broaching: An Extreme Nonlinear Motion Experienced by Small Vessels in Astern Seas"
Thesis submitted for PhD, Australian Maritime College.
- Tuite, A., Renilson, M.R. (1997)
"The effect of principal design parameters on broaching-to of a fishing vessel in following seas"
RINA transactions, spring meetings.
- Umeda, N. (1984),
"Resistance Variation and Surf Riding of a Fishing Boat in Following Seas"
Reprinted bulletin of National Research Institute of Fisheries Engineering, Japan.